

# Robust Stabilization Combining Modal $H_\infty$ Controller for Flexible Rotor Supported by Active Magnetic Bearing

M2016SC003 Masaki GOTO

Supervisor : Isao TAKAMI

## 1 Introduction

The purpose of this study is to control attitude of the rotor which is supported without contact by the active magnetic bearing (AMB). In general, the model of the supported rotor by the AMB is represented as the rigid model [1][2]. However, at the high angular velocity, the resonance must be considered when the controller is designed. Furthermore, the rotor is treated as the flexible rotor to design the controller. Therefore, the finite element method (FEM) is used to derive the mathematical model considering the flexible mode of the rotor [3]. For the derived mathematical model, controller design is difficult because the derived model by using FEM tends high order. Therefore, the order of the derived mathematical model is reduced to design controller easily. The mode transformation is used to reduce the order of the model [4]. The physical coordinates are transformed to the mode coordinates by using the mode transformation. Furthermore, the each resonance mode can be represented by the modal motion. The angular velocity is increased to the operational velocity. In this study, the operational velocity is higher than the 1st resonance frequency. Therefore, the controller considering the rigid mode and the 1st resonance mode is designed.

The major causes of vibration are the gyroscopic effect and the imbalance of the rotor. Here, the gyroscopic effect is proportional to the angular velocity. Furthermore, the force and torque caused by the imbalance are proportional to square of the angular velocity. The vibration caused by the imbalance is represented by the periodic disturbance. When the angular velocity of the rotor which has the imbalance coincides with the natural frequency of the rotor, resonance occurs. Applying balancing to the rotor is one of the method to prevent resonance [5]. However, this paper proposes the control method to suppress the vibration. To design controller is difficult if there exist some varying parameters which depend on the angular velocity of the rotor in the mathematical model because the robust stability must be guaranteed for the prescribed range of the angular velocity. It is well known that the robust stability is guaranteed by the RLQ and  $H_\infty$  control. Especially,  $H_\infty$  control is effective for the periodic disturbance [6].

General procedure of the controller design for the flexible rotor are to derive the mathematical model, to transform the coordinates, to reduce the order and to design the controller. To date, the controllers for the reduced model constructed by the rigid mode and some flexible mode are designed [7][8]. However, the state space representation which has no relationship between the rigid mode and the flexible mode can be derived. Therefore, the controllers designed for the each mode can utilize the their advantages.

In this study, the method of the controller design is proposed such that the controller is made by combining the two controllers after they are designed for the rigid mode and the 1st resonance mode, independently. In the previous study [6], the result is obtained such that the

controller gain derived by  $H_\infty$  controller is higher than the controller gain derived by  $H_\infty$  controller using LFT and descriptor representation. In other words, the high gain controller is effective for the suppressing vibration and the low gain controller is effective for the suppressing the input current. Therefore,  $H_\infty$  controller using LFT and descriptor representation is designed for the rigid mode to suppress the input current and  $H_\infty$  controller is designed for the 1st resonance mode to suppress the vibration, respectively. After that, the controller is designed by coupling these controllers. The effectiveness of the proposed controller is illustrated by the simulation.

## 2 Modeling

Figure 1 shows the flexible rotor. The AMB has four

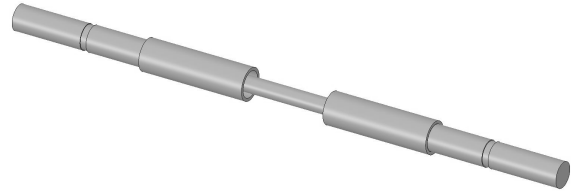


Figure 1 Flexible Rotor

electromagnets and two gap sensors at the both ends of the rotor. The vibration is suppressed by the controlled levitation forces of the electromagnets. To derive the mathematical model of the flexible rotor, FEM is used. From the shape of the rotor illustrated at the Figure 1, a number of elements is defined as 3. The motion equation of the flexible rotor is represented as Eq. (1).

$$M\ddot{q} + J_p p \dot{q} + Kq = f \quad (1)$$

$$q = [q_1 \quad \dots \quad q_3]^T, q_i = [x_i \quad \phi_{xi} \quad y_i \quad \phi_{yi}]^T, (i = 1 \dots 3)$$

Here,  $M$ ,  $J_p$  and  $K$  represent mass matrix, gyro matrix and stiffness matrix, respectively. The displacement of each element and the levitation force are represented as  $q$  and  $f$ , respectively. The levitation force of the electromagnet is given as Eq. (2). Eq. (3) is obtained by the first-order approximation at the equilibrium point because the operating velocity of the AMB dose not vary significantly.

$$f = k_m \left\{ \frac{(B + (I_{x,y} + i))^2}{(q_j - G)^2} - \frac{(B - (I_{x,y} + i))^2}{(q_j + G)^2} \right\} \quad (2)$$

$$f = K_i I_{x,y} + K_{x,y} q + K_i i \quad (3)$$

$$K_{x,y} = k_m \frac{4(B^2 + I_{x,y}^2)}{G^3}, K_i = k_m \frac{4B}{G^2}$$

Here,  $k_m$ ,  $B$ ,  $I_{x,y}$ ,  $i$  and  $G$  represent levitation force constant, bias current, steady current, controlled input current and steady gap between the electromagnet and surface of the rotor, respectively. The controlled input  $u$  is defined as  $u = [\dot{i}_{xl} \quad \dot{i}_{yl} \quad \dot{i}_{xr} \quad \dot{i}_{yr}]^T$ . The term of  $f$  is

represented as following equation.

$$f = (f_x K_x + f_y K_y)q + K_i T_1 u \quad (4)$$

The state space representation at the physical coordinate is shown as follows.

$$\begin{aligned} x_p &= [q_1 \ q_2 \ q_3 \ \dot{q}_1 \ \dot{q}_2 \ \dot{q}_3] \\ \dot{x}_p &= A_p(p)x_p + B_{p1}u + B_{p2}w \end{aligned} \quad (5)$$

$$y = C_p x_p \quad (6)$$

The controller design is difficult because the order of the displacement vector  $q$  is 12, therefore it is transformed by the mode transformation to reduce the order of the model. The mode transformation for the modeling of the flexible rotor is common method and can represent as the modal motion [3]. The transformation matrix  $\Phi$  and the natural frequency of the rotor  $\omega$  can be derived by the eigenvalue analysis for Eq. (1) which has no angular velocity and no force ( $p = 0, f = 0$ ). The transformation matrix is composed by the natural vectors which are obtained by solving generalized eigenvalue problem for the mass matrix and the stiffness matrix. Furthermore, it is normalized by the mass matrix and satisfies  $\Phi^T M \Phi = I$ . Note that, in the eigenvalue analysis, gyroscopic effect is neglected because it is too small. For that reason, mode transformation does not diagonalize strictly the matrix of the gyroscopic effect. The physical coordinates are transformed to the mode coordinates such as  $q = \Phi \zeta$  by the obtained transformation matrix. The state variable is defined as  $x = [\zeta_1 \dots \zeta_{12} \ \dot{\zeta}_1 \dots \dot{\zeta}_{12}]^T$  and we obtain the following state space representation Eq. (7) of the full model.

$$\dot{x} = A(p)x + B_1 u + B_2(p^2)w \quad (7)$$

Here,  $\omega_i (i = 1 \dots 12)$  shows the natural frequencies of the flexible rotor. Especially,  $\omega_5$  and  $\omega_6$  are the 1st resonance frequency. The matrix  $T_1$  and  $T_2$  represent position of the electromagnets and the imbalance, respectively. The state variables represent each mode. For example,  $[\zeta_1 \dots \zeta_4]$ ,  $[\zeta_5, \zeta_6]$  and  $\zeta_i, (i \geq 7)$  mean the rigid mode, the 1st resonance mode and higher order resonance mode, respectively. This study treats the rigid mode and the 1st resonance mode, therefore following reduced model (8) is used.

$$\begin{aligned} \hat{x} &= [\zeta_1 \ \dots \ \zeta_6 \ \dot{\zeta}_1 \ \dots \ \dot{\zeta}_6]^T \\ \dot{\hat{x}} &= \hat{A}(p)\hat{x} + \hat{B}_1 u + \hat{B}_2(p^2)w \end{aligned} \quad (8)$$

Figure 2 shows the bode diagrams of the full model (7)

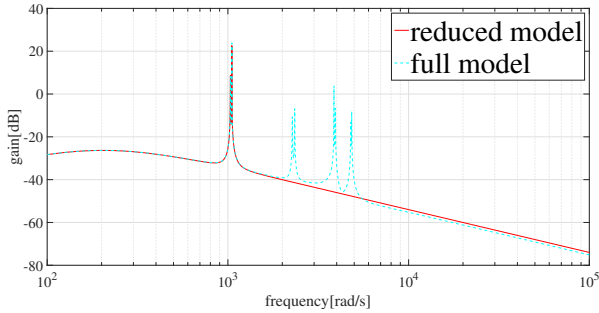


Figure 2 Bode Diagram

and the reduced model (8). From Figure 2, the reduced model has only the rigid mode and the 1st resonance mode. In generally, the controller is designed for the reduced model (8). However, each controller is designed for the rigid mode and the 1st resonance mode, independently in this study. After that, two controllers are combined as the new controller for the reduced model (8). Therefore, the reduced model is divided to the rigid mode (9) and the 1st resonance mode (10). Note that the reduced model can be divided because the all blocks of matrix  $\hat{A}(p)$  in Eq. (8) are the diagonal matrix. In other words, the each mode has no relationship with another mode.

$$\begin{aligned} x_r &= [\zeta_1 \ \dots \ \zeta_4 \ \dot{\zeta}_1 \ \dots \ \dot{\zeta}_4]^T \\ \dot{x}_r &= A_r(p)x_r + B_{1r}u + B_{2r}(p^2)w \end{aligned} \quad (9)$$

$$\begin{aligned} x_f &= [\zeta_5 \ \zeta_6 \ \dot{\zeta}_5 \ \dot{\zeta}_6]^T \\ \dot{x}_f &= A_f(p)x_f + B_{1f}u + B_{2f}(p^2)w \end{aligned} \quad (10)$$

The rigid mode (9) has the second order terms of the angular velocity. To reduce the conservativeness of the matrix polytope, these terms are converted as the first order ones by using LFT and descriptor representation [6]. Therefore, the low conservative controller can be designed for the rigid mode. Eq. (11) is obtained by using LFT for the matrix of the disturbance  $B_{2r}(p^2)$ .

$$B_{2r}(p^2) = B_\delta p(I - D_\delta p)^{-1} C_\delta \quad (11)$$

The descriptor variable  $z_\delta$  and the new state variable  $\hat{x}_r$  are defined as  $z_\delta = (I - D_\delta p)^{-1} C_\delta w$  and  $\hat{x}_r = [x_r \ z_\delta]^T$ , respectively. We obtain the following descriptor system Eq. (12).

$$E \dot{\hat{x}}_r = \hat{A}_r(p)\hat{x}_r + \hat{B}_{1r}u + \hat{B}_{2r}w \quad (12)$$

### 3 Observer design

In this section, the full order observer for the estimation of the displacements is designed because the AMBs has no center at the center of the rotor. Here, the observer is restricted to designing on the discrete time. For the observer design, the dual system is derived from the state space representation at the physical coordinate. The discrete system and the dual system are shown in Eq. (13) and (14), respectively.

$$\begin{aligned} \tilde{x}(k+1) &= \tilde{A}_p \tilde{x}_p(k) + \tilde{B}_{p1} u(k) \\ y(k) &= C_p \tilde{x}_p(k) \end{aligned} \quad (13)$$

$$\begin{aligned} \tilde{A}_p &= e^{A_p T_s}, \tilde{B}_{p1} = \int_0^{T_s} e^{A_p \tau} B_{p1} d\tau \\ x_d(k+1) &= A_d x_d(k) + B_{d1} u(k) \\ A_d &= \tilde{A}_p^T, B_{d1} = C_p^T \end{aligned} \quad (14)$$

Here,  $T_s$  shows the sample time. The observer gain which stabilizes the obtained dual system is derived by the optimal regulator theorem and solving the LMI conditions. The cost function (15) is defined as following equation.

$$J = \sum_{k=0}^{\infty} (x_d(k)^T Q x_d(k) + u(k)^T R u(k)) \quad (15)$$

$$Q > 0, R > 0$$

The observer gain can be obtained by the following Theorem 1.

**Theorem 1** : If there exist matrices  $X_d$  and  $Y_d$  satisfying the following LMI conditions, the system (14) is stabilized by  $u = Y_d X_d^{-1} x_d = K_d x_d$ . Furthermore, the cost function is minimized.

$$\begin{bmatrix} X_d & (A_d X_d + B_d Y_d)^T & X_d Q & Y_d^T R \\ A_d X_d + B_d Y_d & X & 0 & 0 \\ Q X_d & 0 & Q & 0 \\ R Y_d & 0 & 0 & R \end{bmatrix} \succ 0$$

$$X_d = X_d^T \succ 0, \begin{bmatrix} z & I \\ I & X_d \end{bmatrix} \succ 0$$

## 4 Controller design

In this section, the controllers for the rigid mode and the 1st resonance mode are designed. Both modes are stabilized by the state feedback  $u = K_r \hat{x}_r$  and  $u = K_f x_f$ , respectively.

### 4.1 Controller Design for the Rigid Mode

The robust  $H_\infty$  controller for the rigid mode (9) is designed by using the descriptor system (12). The output  $z_r$  is defined as Eq.(16).

$$z_r = W_{sr} \hat{x}_r + W_{ur} u \quad (16)$$

Here,  $W_{sr}$  and  $W_{ur}$  are the weighting matrices for the state variable and the input variable, respectively. The LMI conditions to derive the  $H_\infty$  controller which stabilizes the descriptor system are given as follows [6].

**Theorem 2** : If there exist matrices  $X_r$  and  $Y_r$  satisfying the following LMI conditions, the system (12) is stabilized by  $u = \hat{K}_r \hat{x}_r = Y_r X_r^{-1} \hat{x}_r$  and the system (9) is stabilized by  $u = K_r x_r = Y_{r11} X_{r11}^{-1} x_r$ . Furthermore,  $H_\infty$  norm is less than  $\gamma_{r\infty}$ .

$$\begin{bmatrix} He[M_r(p)] & \hat{B}_{2r} & (W_{sr} X_r + W_{ur} Y_r)^T \\ \hat{B}_{2r}^T & -\gamma_{r\infty}^2 I & 0 \\ W_{sr} X_r + W_{ur} Y_r & 0 & -I \end{bmatrix} \prec 0 \quad (17)$$

$$M_r(p) = \hat{A}_r(p) X_r + \hat{B}_{1r} Y_r, Y_r = \hat{K}_r X_r \quad (18)$$

$$X_r = \begin{bmatrix} X_{r11} & 0 \\ X_{r12} & X_{r22} \end{bmatrix}, X_{r11} \succ 0, Y_r = [Y_{r11} \quad 0] \quad (19)$$

To guarantee the robust stability for the varying angular velocity  $p \in [p_1, p_2]$  of the rotor of the system (12), the LMI condition (17) must be satisfied for all  $p \in [p_1, p_2]$ . This means that, the infinite set of LMI conditions have to be solved. To avoid this problem, the matrix  $\hat{A}_r(p)$  is represented as Eq.(20) by the matrix polytope.

$$\hat{A}_r(p) = \lambda \hat{A}_r(p_1) + (1 - \lambda) \hat{A}_r(p_2) \quad (0 \leq \lambda \leq 1) \quad (20)$$

If the LMI condition (17) is satisfied at the both vertex matrices  $\hat{A}_r(p_1)$  and  $\hat{A}_r(p_2)$ , the stability is guaranteed for all angular velocity. The common solution is obtained by solving the following set of LMI conditions shown in Corollary 1 [6].

**Corollary 1** : If there exist matrices  $X_r$  and  $Y_r$  satisfying the following LMI conditions and (19), the system (12) is stabilized by  $u = \hat{K}_r \hat{x}_r = Y_r X_r^{-1} \hat{x}_r$  for the prescribed range of angular velocity  $p$ . Furthermore,  $H_\infty$

norm is less than  $\gamma_{r\infty}$ .

$$\begin{bmatrix} He[M_r(p_i)] & \hat{B}_{2r} & (W_{sr} X_r + W_{ur} Y_r)^T \\ \hat{B}_{2r}^T & -\gamma_{r\infty}^2 I & 0 \\ W_{sr} X_r + W_{ur} Y_r & 0 & -I \end{bmatrix} \prec 0 \quad (i = 1, 2) \quad (21)$$

### 4.2 Controller Design for the 1st Resonance Mode

To suppress the vibration around the 1st resonance frequency, the robust  $H_\infty$  controller for the 1st resonance mode (10) is designed. The output  $z_f$  is defined as Eq.(22).

$$z_f = W_{sf} x_f + W_{uf} u \quad (22)$$

The robust stability for the varying parameter  $p$  must be guaranteed as same as the rigid mode. Therefore, the vertex matrices are represented as  $A_f(p_1)$ ,  $A_f(p_2)$ ,  $B_{2f}(p_1^2)$  and  $B_{2f}(p_2^2)$  by the matrix polytope. The controller can be designed if the following LMI conditions are solved at the vertex matrices shown in Theorem 3.

**Theorem 3** : If there exist  $X_f$  and  $Y_f$  satisfying the following LMI conditions, the system (10) is stabilized by  $u = K_f x_f = Y_f X_f^{-1} x_f$ . Furthermore,  $H_\infty$  norm is less than  $\gamma_{f\infty}$ .

$$\begin{bmatrix} He[M_f(p)] & B_{2f}(p^2) & (W_{sf} X_f + W_{uf} Y_f)^T \\ B_{2f}(p^2)^T & -\gamma_{f\infty}^2 I & 0 \\ W_{sf} X_f + W_{uf} Y_f & 0 & -I \end{bmatrix} \prec 0 \quad (23)$$

$$M_f(p) = A_f(p) X_f + B_{1f} Y_f, Y_f = K_f X_f \quad (24)$$

$$X_f \succ 0 \quad (25)$$

Note that, to guarantee the robust stability, the LMI conditions are solved at the three vertex matrices.

### 4.3 Stabilization for the Reduced System

The goal is to stabilize the system (8) by  $u = [K_r \quad K_f] [\hat{x}_r^T \quad x_f^T]^T$ . However, both systems use same input. Therefore, each input affect to another state as a disturbance. As a result, stability may be lost. To guarantee the stability, other LMI conditions are added by the Theorem 4.

To derive the LMI condition to guarantee the stability, following system is considered.

$$\begin{bmatrix} E & 0 \\ 0 & I \end{bmatrix} \begin{bmatrix} \hat{x}_r \\ x_f \end{bmatrix} = \begin{bmatrix} \hat{A}_r(p) & 0 \\ 0 & A_f(p) \end{bmatrix} \begin{bmatrix} \hat{x}_r \\ x_f \end{bmatrix} + \begin{bmatrix} \hat{B}_{1r} \\ B_{1f} \end{bmatrix} u + \begin{bmatrix} \hat{B}_{2r} \\ B_{2f} \end{bmatrix} w \quad (26)$$

**Theorem 4** : If there exist matrices  $X_r$ ,  $X_f$ ,  $Y_r$  and  $Y_f$  satisfying the following LMI conditions, the system (26) is stabilized by  $u = [K_r \quad K_f] [\hat{x}_r \quad x_f]^T$ .

$$\begin{bmatrix} He[M_r(p)] & (B_{1f} Y_r)^T + B_{1r} Y_f \\ B_{1f} Y_r + (B_{1r} Y_f)^T & He[M_f(p)] \end{bmatrix} \prec 0 \quad (27)$$

$$P_{11}^{-1} = X_r, P_{22}^{-1} = X_f \quad (28)$$

The combined controller can be designed if the LMI conditions (21), (23) and (27) are solved.

## 5 Simulation

The effectiveness of the proposed controller is illustrated by simulation comparing with the conventional robust  $H_\infty$  controller. The LFT is used for the both model rigid mode and 1st resonance mode when the conventional controller is designed. In these simulations, the correctness of the comparison is guaranteed by using same weights for the state variable and the input variable when the controllers are designed. The parameters of the control target is used as the example value. From the eigenvalue analysis, the 1st resonance frequency is derived as 1041.7 [rad/s]. The initial angular velocity and the initial angular acceleration are set up as 0 [rad/s] and 26.1[rad/s<sup>2</sup>], respectively. The results of simulations are shown in following figures. Figure 3 illustrates the position displacement of the center

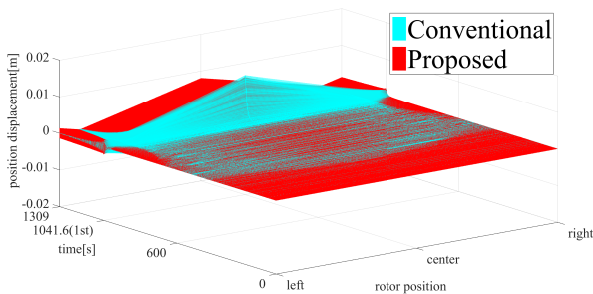


Figure 3 Position displacement

of the rotor. Figure 4 illustrates the input current of

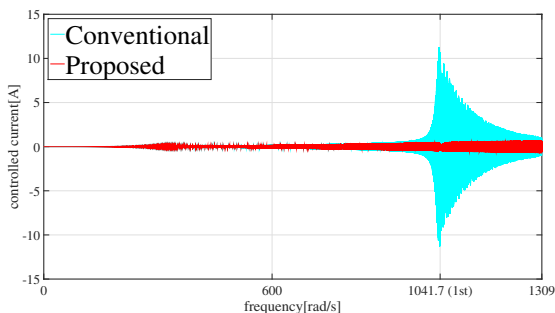


Figure 4 Input current

the electromagnetic which set at the vertical direction of the right side. From Figure 3, up to the 1st resonance frequency, the proposed controller can suppress the vibration as same as the conventional controller. The convergence performance of the conventional controller is better than the proposed controller. However, the conventional controller use the current higher than limit of the AMBs. These results show the effectiveness of the proposed method.

## 6 Experiment

In this section, the effectiveness of the proposed method is checked by the experiment. The angular velocity is set as about 600 [rad/s]. The proposed controller is implemented to the left side of the AMBs. The right side of the AMBs is controlled by the internal controller. The experiment results are shown as follows.

Figure 5 shows the position displacement of the rotor

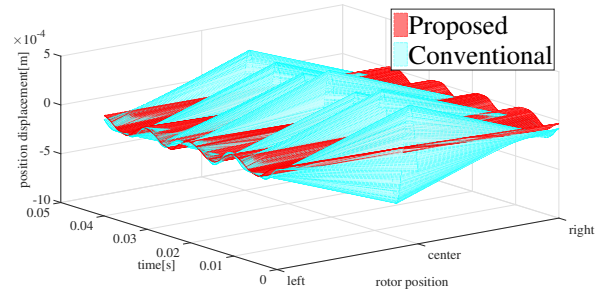


Figure 5 Position displacement

on the vertical direction. The AMBs has no sensor at the center of the rotor. Therefore, the estimated state is illustrated. From Figure 5, the vibration is more suppressed by proposed controller. The rotor is bending when the conventional controller is applied, however, the bending of the rotor dose not generate.

## 7 Conclusion

In this paper, the method of the controller design for the modal vibration is proposed. This mean that the controller is not directly designed for the reduced model of the flexible rotor. Advantage of the proposed method is that the controller for each mode can be designed by dividing the reduced model into the rigid mode and the flexible mode. In my previous study, there are tendency like that the  $H_\infty$  controller and the  $H_\infty$  controller using LFT and descriptor representation have advantages of suppressing vibration and input current, respectively. The proposed controller include these advantages. However, to design the  $H_\infty$  controller using LFT and descriptor representation is not effectiveness for the flexible mode. In the designing controller, the stability can not be guaranteed by simply combined controller. Therefore, to guarantee the stability, the LMI condition is added. The effectiveness of the proposed method is illustrated by simulation and experiment.

## References

- [1] F. Matsumura, T. Namerikawa, K. Hagiwara and M. Fujita, "Application of Gain Scheduled  $H_\infty$  Robust Controllers to a Magnetic Bearing", IEEE Transaction on Control Systems Technology, Vol.4, No.5, 1996.
- [2] A. Sanbayashi, M. Narita, G. Chen and I. Takami, "Gain Scheduled Control for Active Magnetic Bearing System Considering Gyroscopic Effect", Proc. 2015 7th International Conference on Information Technology and Electrical Engineering, pp. 553-558.
- [3] K. Nonami and T. Ito, " $\mu$  Synthesis of Flexible Rotor-Magnetic Bearing Systems", IEEE Transaction on Control Systems Technology, Vol.4, No.5, 1996.
- [4] Y. Zhang, K. Nonami, N. Kobayashi, M. Ren, A. Kubo and R. Takahata, "Zero Power Control of Energy Storage Flywheel System Using Cholesky Decomposition with Gyroscopic Effect" (in Japanese), Transactions of the Japan Society of Mechanical Engineers Series C, Vol. 70, No. 698, pp. 2805-2811, 2004.
- [5] S. Edwards, A. W. Lees and M. I. Friswell, "Experimental Identification of Excitation and Support Parameters of a Flexible Rotor-Balancing-Foundation System from a Single Run-Down", Journal of Sound and Vibration, Vol. 232(5), pp. 963-992, 2000.
- [6] M. Goto, T. Mizuno, G. Chen and I. Takami, "Robust  $H_\infty$  control for Active Magnetic Bearing system with imbalance of the rotor", 2016 IEEE 14th International Workshop on Advanced Motion Control (AMC), pp. 297-303, 2016.
- [7] K. Nonami and H. Tian, "Sliding Mode Control of Flexible Rotor-Magnetic Bearing Systems Using Robust Reduced-Order VSS Observer" (in Japanese), Transactions of the Japan Society of Mechanical Engineers Series C, Vol. 60, No. 571, pp. 897-905, 1994.
- [8] N. Takahashi, O. Matsushita and M. Takagi, "Control of Flexible Rotors Supported by Active Magnetic Bearings" (in Japanese), Transactions of the Japan Society of Mechanical Engineers Series C, Vol. 61, No. 588, pp. 3228-3233, 1995.